

Full Length Research Paper

***In silico* design of cyclic peptides as influenza virus, a subtype H1N1 neuraminidase inhibitor**

Usman Sumo Friend Tambunan*, Noval Amri and Arli Aditya Parikesit

Department of Chemistry, Faculty of Mathematics and Science, University of Indonesia, Depok, 16424 Indonesia.

Accepted 4 June, 2012

Nowadays, influenza has become a global public health concern because it is responsible for significant morbidity and mortality due to annual epidemics and unpredictable pandemics. There are only limited options to control this respiratory disease. Vaccine treatment is useless for controlling this disease because of the occurrence of mutation in the influenza virus. Influenza virus is also resistant to some antiviral drugs like oseltamivir and zanamivir, which inhibit neuraminidase. Another solution for controlling this virus is to find new design for antiviral drugs. Cyclic peptides can be used to make new antiviral drug design especially to inhibit neuraminidase activity by using 'structure-based design' method. Based on molecular docking, new antiviral drug designs have been found. They are DNY, NNY, DDY, DYY, RRR, RPR, RRP and LRL. These cyclic peptides showed better activity and affinity than standard ligand to inhibit neuraminidase activity. From drug scan, DNY, NNY and LRL ligands have low toxicity and were predicted to have at least 59% possibility that it could be synthesized in wet laboratory experiment.

Key words: Influenza virus A, neuraminidase, cyclic peptide, structure based design, molecular docking.

INTRODUCTION

Influenza is a contagious disease caused by viruses that infect humans and animals. In general, influenza is a virus that spreads among certain species. It means, when the virus infects one species, it rarely infects other species. General symptoms of the disease include fever, headache, sore throat and cough. Several serious cases of influenza could lead to pneumonia and end with mortality (Kamps et al., 2006). Influenza virus is part of the order mononegavirales and family of orthomyxoviridae, which has a genome with single segment. On the basis of its genus, there are three types of influenza viruses: type A, B and C. Influenza A and B viruses have 8 ribonucleic acid (RNA) segments, while type C has seven RNA segments. Nucleic acid of influenza virus was translated to about 10 proteins, haemagglutinin (HA), neuraminidase (NA), matrix protein (M1 and M2), non-structural proteins (NS1 and NS2), nucleocapsid protein (NP), polymerase basic (PB1 and PB2), and polymerase acidic (PA) (De Jong et al., 2005).

Based on its antigenic properties, influenza virus has two surface functional glycoproteins. They are HA, NA and the M2 proton channel. H1N1 subtype is a virus that belongs to the influenza virus type A. This type of virus is composed of 16 HA (H1-H16) and 9 NA (N1-N9). Theoretically, there are 16 × 9 subtypes, and until now 105 subtypes of influenza A viruses have been found. They are all endemic in birds. However, several subtypes have been found in chickens and mammals (Michaelis et al., 2009). The long-sought 3D structures of the M2 proton channels for influenza A (Schnell et al., 2008) and B (Wang et al., 2009) viruses were successfully determined by the high-resolution nuclear magnetic resonance (NMR) spectroscopy. Pielak and Chou (2010) have emphasized, that histidine protonation and opening of the channel gate are synchronized events. Pielak et al. (2009) underlined that drug-resistant mutants impair drug binding by destabilizing M2 helix-helix assembly. Du et al. (2009) argued that energetics, the channel-gating dynamic process, the pK(a) shift, its impact on the channel and the consistency with the previous functional studies, among others, are in favour of the allosteric mechanism revealed by the M2 NMR structure. Those

*Corresponding author. E-mail: usman@ui.ac.id.

findings may stimulate and encourage new strategies for developing effective drugs against influenza A, particularly in dealing with the drug-resistant problems. Moreover, Du et al. (2010) also underlined that the newly designed adamantane-based inhibitors based on the modeled structure of H1N1-M2 proton channel have two pharmacophore groups, which act like a 'barrel hoop' holding two adjacent helices of the H1N1-M2 tetramer through the two pharmacophore groups outside the channel.

Huang et al. (2008) have performed in-depth analysis for M2 functional studies, particularly for the mutations D44N, D44A and N44D on position 44, and the mutations on positions 27 to 38. Wang and Chou (2010) have proved that the molecular dynamic simulated structures of M2 that the mutant channel could still open even if binding with rimantadine, but the wild type channel could not. Wang et al. (2009) have found that amantadine and rimantadine binding affinity to the H1N1-M2 channel is significantly lower than that of the H5N1-M2 channel. This is fully consistent with the recent report that the H1N1 swine virus was resistant to the two drugs. Wei et al. (2009) have found that a benchmark data set has been constructed containing 34 newly-developed adamantane-based M2 inhibitors and covers considerable structural diversities and wide range of bioactivities. Such milestone works provides a solid structural basis for in-depth understanding of the action mechanism of the M2 channel and rationally design effective drugs against influenza viruses. During the 20th century, influenza virus type A was a scary pandemic disease. Three occurrences of pandemic influenza have caused millions of deaths. Occurred pandemic (Spanish flu) in 1918 to 1919 was caused by the H1N1 subtype, and caused 50 million deaths. The second pandemic (Asian flu) in 1957 to 1958 was caused by the H2N2 subtype and caused one million deaths. The third pandemic (Hong Kong flu) in 1967 to 1968 was caused by the H3N2 subtype and caused one million deaths (Kamps et al., 2006). In the year 2009, a new strain of H1N1 has been discovered. It is known as the Mexican influenza (swine flu) (Michaelis et al., 2009). The virus is a combination of gene segments of influenza viruses from pigs, birds and humans (Rungrotmongkol et al., 2009).

One of the prevention of H1N1 virus infection is by vaccination, although, present vaccines are considered to have fewer efficacies in protecting the body when the influenza virus infects it (Tomassini et al., 1994). This is caused by a mutation of the virus (antigenic drift) or antigenic shift that can occur when a cell is infected with two types of viruses that are still in one family (Kamps et al., 2006). At this time, drugs have been developed as an antiviral instead of vaccines. One of antiviral commercial products, which can inhibit the development of the H1N1 virus, is the NA inhibitor, oseltamivir and zanamivir. Both of these antiviral medications were recommended by the Centers of Disease Control and Prevention (CDC) and

World Health Organization (WHO) (Rungrotmongkol et al., 2009). It is considered effective in treating influenza virus infection that occurs in humans (Lew et al., 2000). In addition, there are adamantine antiviral, amantadine and rimantadine which can inhibit M2 ion-channel (De Clercq, 2006).

However, the virus resistance to these drugs had occurred because of mutations (Beigel et al., 2005; De Jong et al., 2005). Research groups in the world have been trying to discover the most effective drugs against H1N1. Li et al. (2011), searching for zinc fragment database, found that Neo6 compound is a good lead compound. Qu-shi et al. (2009) try to elucidate drug-protein structural features of NA and M2 protein and annotate its residual mutation. Wang et al. (2009) investigated the drug-resistance tendency of oseltamivir towards H5N1 and generated valuable data for designing H1N1 drugs. Du et al. (2007) proposed six analog inhibitors as candidates for developing inhibitors against H5N1 virus. Gong et al. (2009) found that the compound AG7088 has better binding energy than zanamivir and oseltamivir and nine analogs of AG7088 were singled out through a series of docking studies. Guo et al. (2008) found that some mutations of H5N1 H5 cleavage sequence fitted less well into furin and would reduce high pathogenicity of the virus. These findings hint that we should focus on the sub-sites P (1), P (4), and P (6) for developing drugs against H5N1 viruses. Wang et al. (2007), while trying to find the possible drug-resistant H5N1 virus by conducting similar analysis using the BAE46950 sequence (homology model of H5N1-NA) as the benchmark template, 21 sequences were found from the database of the 108 H5N1 NAs that had over 95% sequence similarity with BAE46950.

Wei et al. (2006) found subtle mutated variations that not only destroy the original lipophilic environment of the H5N1-NA and 2,3-didehydro-2-deoxy-N-acetylneuraminic acid (DANA), but also change its complement interaction. Therefore, such findings might provide insights into the secret why some of H5N1 strains bear high resistance against existing NA inhibitors. Wang et al. (2010) found three lead compound derivatives that formed stronger inhibition power than oseltamivir; hence, they may become excellent candidates for developing new and more powerful drugs for treating influenza. Du et al. (2011) argued that structure-based drug design is the inventive process for finding new drugs based on the structural knowledge of the biological target. Many studies have indicated that computational approaches, such as predicting drug-target interaction networks (He et al., 2010), predicting human immune virus (HIV) cleavage sites in proteins (Chou, 1993, 1996), prediction of body fluids (Hu et al., 2011), predicting protein metabolic stability (Huang et al., 2010), predicting signal peptides (Chou and Shen, 2007), predicting the network of substrate-enzyme-product triads (Chen et al., 2010), predicting protein subcellular locations (Chou and Shen,

2008; Chou et al., 2011), predicting proteases and their types (Chou and Shen, 2008), predicting antimicrobial peptides (Wang et al., 2011), predicting membrane proteins and their types (Chou, 2001; Chou and Shen, 2007), predicting G protein coupled receptors (GPCRs) and their types (Xiao et al., 2011), identifying nuclear receptor subfamilies (Wang et al., 2011), predicting biological functions of compounds based on chemical-chemical interactions (Hu et al., 2011), and predicting transcriptional activity of multiple site p53 mutants (Huang et al., 2011) can provide many useful insights and data which would be time-consuming and costly to obtain by experiments alone.

Actually, these data, combined with the information derived from the structural bioinformatics tools (Chou, 2004; Chou et al., 2003), can timely provide very useful insights into both basic research and drug development. In view of this, the present study is an attempt to use computational approaches for finding novel inhibitors against influenza. We hope that our findings may be useful for drug development. Computational docking operation is a useful vehicle for investigating the interaction of a protein receptor with its ligand and revealing their binding mechanism as demonstrated by a series of studies (Chou et al., 2003, Huang et al., 2008; Wang et al., 2009; Du et al., 2009; Wei et al., 2009; Du et al., 2010; Wang et al., 2009), The research results of previous groups are our main motivation to study H1N1 drug design. The objective of our research is to discover novel drugs for H1N1, by using cyclic peptide neuraminidase inhibitor.

MATERIALS AND METHODS

Sequence alignment and homology modeling

H1N1 influenza sequences used in this study were downloaded from the NCBI database and from 2009 to 2010 infection. Multiple sequence alignment method was done, using ClustalW2 program and progressive pair wise alignment algorithm (Thompson et al., 1994). 3ckzA was used as a template to build the NA structure using Swiss-model software online workspace (Swiss Institute of Bioinformatics and the Biozentrum University of Basel) by inserting the downloaded FASTA files.

Determination of neuraminidase active site

After obtaining the tertiary structure of the NA protein of influenza virus subtype H1N1, then analysis was performed to determine the active site or binding group of proteins. The coordinates of the active site were determined using Q-site finder online software that can be accessed by <http://bmbpcu36.leeds.ac.uk/qsitfinder/> address. Input data for this program were obtained, using the protein data bank (PDB) format by entering the PDB code or PDB file.

Amino acid sequence determination of peptide inhibitors

Determination of amino acid sequences was used to construct Cyclic peptide based on the analysis result. Disulfide bond was

achieved by joining cysteine residue and these ligands were compared to natural substrate of sialic acid and standard NA inhibitors, oseltamivir and zanamivir, which are widely used.

Dimensional structures design of cyclic peptide ligand

Cyclic peptide was designed and modeled into three-dimensional (3D) structure using ACDlabs software. Cyclic peptide was made in zwitter ion form. Cyclic peptides from three dimensional designs were stored in MicroStation Development Language (MDL) format. It would be converted into cyclic peptide VegaZZ PDB format, and then converted into Pdbqt autodock using software tools.

Determination of grid box

Grid box is a necessary parameter in the process of ligand docking with the target enzyme. Grid box consists of a grid box center and its sizes are determined by looking at the coordinates of the target enzyme active site, using the aid of software tools autodock.

Preparation of file docking

Preparation was conducted by converting the file docking ligands into Pdbqt file format and targeting the enzyme before it was converted. First, the polar hydrogen is added by using software tools autodock.

Processes with target enzyme ligand docking

Docking process is performed using software Autodock vina 1.0 by applying the appropriate parameters.

Analysis of docking results

Analysis of docking results was done by using software MOE 2008.10 and PyMol by looking at certain parameters such as binding affinity, inhibition constant/dissociation (K_i) and corresponding interaction.

Drug scan

Drug scan was performed on the best ligand that has low ΔG° binding and good interaction with the target enzyme. Analysis of drug scans was performed by considering the rules of good medicine (Lipinski's rule of five) and the oral bioavailability of these ligands.

Visualization of enzyme-ligand complex interactions

Visualization of enzyme-ligand: the enzyme-ligand complexes formation was performed using PyMol software for 3D visualization and MOE 2008.10 software for visualization in two-dimensional form.

Toxicological properties

Toxicological properties of best ligand were performed using Lazar ToxTree software and toxicological properties.

Synthetic accessibility prediction

Ligands that show good affinity toward target enzyme do not have a practical value if they could not be synthesized by wet lab. Therefore, to predict whether a designed molecules/ligands can be synthesized, parameter called synthetic accessibility (SA) was utilized. It was provided by online software that helps to determine SA, computer assisted estimation of synthetic accessibility (CAESA). CAESA is developed by Symbiosis Inc. and supported by KeyModule Ltd, Leeds, UK and Pfizer.

RESULTS AND DISCUSSION

Determination of NA sequence

NA sequence that will serve as a target enzyme was determined by using influenza database contained in the NCBI database. Used parameters among other things are NA protein sequences between the years, 2009 to 2010 in all countries, the human host, strain/subtype H1N1. We obtained 241 NA protein sequences from various countries. Multiple alignments between sequences were performed to find sequences that represent existing NA protein from 2009 to 2010. Online clustalW2 software from the official entry blockers (EB) site was used to find the similarity score of each sequence comparison with the highest score being 100. The chosen NA protein sequences are the ones that have the highest similarity value (100). NA protein sequence from Auckland in 2009, NA [A/Auckland/1/2009 (H1N1)] with code ACR08499.1 GenBank was the result.

Preparation of NA 3D structure

Previously determined NA protein sequence with the FASTA file format was downloaded and used as input for Swiss-model software online (Swiss Institute of Bioinformatics and the Biozentrum University of Basel) to get NA protein model. The result is the 3D structure file formats PDB, which is a result of comparison with a template (structural benchmark) from the official site database PDB. One condition that must be considered from the obtained results is that the percentage of identity (% identity) must be at least 60% of the structures made with the compared template. In this case the NA protein 3D structure is 91.123% identical with the template used.

Determination of the NA active side (active site/catalytic site)

Information of NA active site residues was obtained from NCBI. It was performed by searching Gen bank flat file (GBFF) for the utilized sequences by entering codes from the ACR08499.1 GenBank sequence. From the information, seven amino acid residues in the active site are Arg118, Asp151, Glu278, Arg 293, Arg368, Tyr402 and

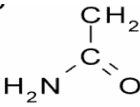
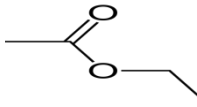
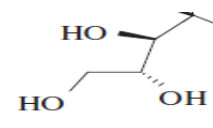
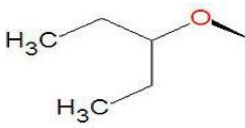
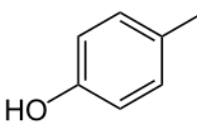
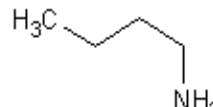
Glu245. These seven amino acid residues are targets for docking process. After detecting amino acid residues on the NA active side, then the determination of the coordinates of the active site was performed. This is shown by the position coordinates X, Y, and Z which will be used in the docking process. This determination is performed using online software Q-sitefinder (<http://bmbpcu36.leeds.ac.uk/qsitefinder/>) by uploading files to the format of the PDB 3D structure, which has been obtained from the 3D structure of NA-making stage. This determination is done by looking at the location of amino acid residues of the NA that we get and the software will display the minimum and maximum coordinates of the areas that have amino acid residues that have been selected. The results of this determination of the minimum (-38, -66 and 3) and maximum (-21, -51 and 19) coordinates from the active site of the coordinates used are the coordinates of the average of the minimum and maximum coordinates of X = -29.5, Y = -58 and Z = 10.5.

Cyclic peptide amino acid sequence determination as inhibitors

The determination of amino acid sequences of peptides as inhibitors in this study is based on the analysis conducted on the structure of the natural substrate of the NA of sialic acid and the antiviral drug that has been used as oseltamivir. From studies conducted by Kubinyi (1998), determination of inhibitor design through this approach is called 'structure-based design' or the determination of the new-inhibitors design with similar structures. This case is seen within the structure of the natural substrate of sialic acid and NA oseltamivir antiviral drug as one that has been used. In this analysis, the determination was made by examining groups that have been shown to have interaction with amino acid residues on the active side of the NA. It is based on studies conducted by Zhang et al. (2009).

From Table 1, the first group on the natural substrate of NA (sialic acid) is the same as oseltamivir's asetamide, while on the design of new inhibitors asetamine is used, which is the side chain of the amino acid asparagine (Asn/N). Asetamine is expected to have better interaction than asetamide because amines have more donated electrons compared to amides. The second group of sialic acid is the carboxyl, while on oseltamivir; it has been modified to be etoxycarbonyl on the design of new inhibitor with sialic acid, which is the carboxyl side chain of amino acids aspartic acid (Asp/D). The third group of sialic acid is a triplet, whereas oseltamivir is utilizing pentiloxy group. The results of the analysis are according to Zhang et al. (2008). This group has the interaction of NA hydrophobic region, on the basis that the design of new inhibitors of the phenolic group was chosen because the structure of benzene is expected to fill the hydrophobic region. It will be further analyzed whether it has effect on its interaction with NA or otherwise adversely

Table 1. Similarity between the group structure of the natural substrate (sialic acid), existing antiviral drugs (oseltamivir) and a new inhibitor.

Sialic acid	Oseltamivir	New-inhibitor
NHCOCH_3	NHCOCH_3	
HO_2C		HO_2C
		
OH	NH_2	

affects its interaction with the NA. Amino acids used for this third group is tyrosine (Tyr/Y) which has a phenol side chain. The last or fourth group of sialic acid is hydroxyl, while for oseltamivir and designs of new inhibitors are amines which have more polarity than hydroxyl, which is expected to have better interaction with the NA. The selected amino acid is lysine (Lys/K) which has the amine group with a four-carbon chain, while on oseltamivir it is not. In studies conducted by Zhang et al. (2009) and Rungrotmongkol et al. (2009), amine group in oseltamivir cannot interact well with acids in the NA active side because it is quite far from NA active side amino acid residues. The expected amine group on lysine, which has four carbon chains, could reduce the interaction distance with the amino acid residues of the active side, causing NA interaction well placed than the amine group of oseltamivir.

Basis for determining the amino acid peptide that would serve as the design of new inhibitor is the one that has been studied by Jones et al. (2006), called entry blockers (EB). It is proven by *in vivo* means that it could act as an inhibitor to reduce the spread of influenza virus infection in testing animals' cell. Although it has been known that influenza virus protein on the surface that serves to bind to host cells is not the HA or NA enzyme targeted in this study, the natural substrate of HA and NA are the sialic acid. Thus, the hypothesis is that the EB amino acid residues have the potential to be an inhibitor of NA and HA. Amino acid composition residue of the EB consists of six amino acids- arginine-lysine-alanine-valine-leucine-proline (RKAVLP).

Design of three-dimensional structure of cyclic peptides ligands

New inhibitors that will be determined in this study will be called ligands. The design of this ligand was done using amino acid residues that had been pre-determined at the determination stage of the peptides amino acid sequences as inhibitors. Amino acid residues are:

1. Based on the similarity properties of clusters (structure based design): asparagine-lysine-tyrosine- aspartic acid (NKDY).
2. Based on the entry blocker (entry blocker-based design): Arginine-lysine-alanine-valine-leucine-proline (R-KAVLP).

Both amino acid residues will be designed to be cyclic peptides with two disulfide bonds using cysteine residues at the ends. Preparation of cyclic peptide was aimed to avoid cutting peptide bonds by proteases that exist in the human body. This is because they recognize only linear form peptide whereas the cyclic peptides cannot be recognized by them. Cyclization is not done by forming a peptide bond at the end of the C and N terminals because cyclization by disulfide bonds provides better stability. Cyclization by disulfide bond can enhance the interaction of hydrophobic peptides and reduce hydrogen interactions with other solvent (water), thus increasing the total entropy and the stability of the peptide.

Designed cyclic peptides are a combination of three amino acid residues with two cysteines (C) end. As shown in Figure 1, cyclic peptide is designed in the



Figure 1. Example of cyclic peptide designs, C is a cysteine.

pentacyclic form because it is more stable than tricyclic or butacyclic. If they are designed to be the circumference of six or hexacyclic (although formed cyclically stable), then it would be having large molecular mass that would affect the results of drug or drug likeness scan. Binghe et al. (2005) stated that there is enzymatic activity of luminal fluid in the stomach and duodenum, whereas the straight peptide of the large size will experience proteolysis. The design of cyclic peptides as ligands was done by using offline chem sketch software (ACD Labs). The results of this design are obtained from the combination of ligand functional groups based on similarity of as many as 64 combinations of ligand and based on a combination of 180 entry-blocker ligands. The subsequent discussion of the design of new ligands is displayed by three constituent amino acid codes (example: DNY).

Determination of grid box

Grid box is the location where the ligands interact with the residue on the target enzyme and is described in the form of a cube. The determination of the grid box is done by using offline autodock software tools with respect to the first two parameters which are the size of the grid box and the second is the initial location of ligand docking called the center. Ligands used for the initial position coordinates of the active side of the NA that had been predetermined at the stage of determining the active side of the NA include the coordinates of X = -29.5, Y = -58; Z = 10.5. As for the size or the size of the grid box, it can be determined manually according to the active side of the majority of the NA. In this case, the measures used are X = 26; Y = 26; Z = 26 with a spacing of 1 Å.

Docking

Conducted docking process in this study was the semi-oriented process by using flexible ligands. It uses the default number of rotatable bond or bonds that can rotate on the ligand set automatically by using software tools autodock. While, the target enzymes that are used for the docking process are made rigid. If both are made flexible, the processes required for the calculation of one-time docking can take a long time. Software used for the docking process is free software autodock vina 1.0, published by the Scripps research institute. Some things

should be prepared prior to docking, which include:

1. Ligand with a Pdbqt format file.
2. Enzyme with a Pdbqt format file.
3. Grid box (centers and size).

Docking process here can only be run through command prompt by using the configuration set by the software. In addition the enzyme and ligand file should be stored in same folder on a computer while the grid box entered manually as the configuration of the docking process to be performed. The time needed for the docking process depends on the size and number of degrees of torsional ligands used in the docking process. The greater the numbers of degrees of torsional to a ligand docking is, the longer the process and vice versa. In this study the time required for one-time docking is about 10 to 15 min.

Determination of enzyme-ligand complex conformation docking results

Determination of conformation of the enzyme-ligand complex docking results is done by selecting a ligand conformation with the best binding affinity ΔG° value (kcal/mol) or the smallest one (best mode). The results of docking software autodock vina 1.0 are the best conformation of nine enzyme-ligand complexes. They are selected with the Pdbqt file format. Those overall conformations of the enzyme-ligand complexes that can happen are based on the degree of torsional ligand. While the results of calculations ΔG° binding affinity (kcal/mol) can be seen in the log file that can be opened by using text editor.

The standard ligand docking

Strength inclination of the bond can be referred to as the affinity of the ligand to a receptor or enzyme. It can be determined by looking at the ΔG° binding affinity (kcal / mol) value generated during the formation of enzyme-ligand complexes. High affinity of a ligand to an enzyme is produced from a large intermolecular force between the ligand with the enzyme, whereas the low affinity of a ligand to an enzyme is produced from a small intermolecular force between them. If the affinity of a ligand to the enzyme is higher then the value ΔG° binding affinity (kcal / mol) will be lower. On the contrary, if affinity gets smaller then the value ΔG° binding affinity (kcal / mol) increases. This also affects the residence time of ligand binding with the enzyme. If the affinity of a ligand to an enzyme is better then residence time of ligand binding to the enzyme is also getting better. The followings are the results of binding energy and the contact residues of the used ligand. From the results shown in Table 2, it can be seen that oseltamivir has the

Table 2. Energy bonds and the contact residues of the standard ligand.

No.	Standard	ΔG° binding affinity (kcal/mol)	Contact residuer
1	Oseltamivir	-6.5	TYR 402, ARG 293
2	Zanamivir	-7.4	ASP 151, ASP 151, TRP 179, GLU 278, TYR 402, ARG 368, TYR 402, TYR 402
3	Sialic acid	-7.1	GLU 277, GLU 278, TYR 402, ARG 225, ARG 293, ARG 293, ARG 293, TYR 402
4	DANA	-6.7	ASP 151, GLU 277, GLU 278, GLU 278, TYR 402, ARG 293, TYR 402, TYR 402
5	RWJ-270201	-6.8	ASP 151, TRP 179, GLU 278, ARG 156

Bold print is the targeted residue.

concluded that the NA would be more likely to bind sialic acid in comparison with oseltamivir whereas zanamivir has the smallest ΔG° binding affinity value of -7.4 Kcal/mole. In other words, the affinity of zanamivir against NA is the highest compared with other standards or even with sialic acid as NA natural substrate.

Theoretically, NA would be more likely to bind with zanamivir than sialic acid. DANA is an inhibitor that is used to inhibit NA before zanamivir was found. It has ΔG° binding affinity value of -6.7 Kcal/mole; the value is greater than zanamivir and sialic acid. The mean affinity of NA-DANA is lower compared to zanamivir and sialic acid. That is similar with RWJ-270 201, which was computed previously (Young et al., 2001). RWJ-270 201 has a better activity than oseltamivir. However, the result of the ΔG° docking binding affinity, despite its value being smaller than oseltamivir, is still larger when compared with the sialic acid. RWJ-270 201 has a lower affinity than the sialic acid, and theoretically sialic acid would be more likely to bind to NA. The occurring contact residues showed that interaction of NA with oseltamivir is not good enough because only two contact residues occurred. It is possible to occur because of amino acid residues mutations at the NA or influenza virus strain used is as a result of reassortment or merging of two different influenza virus strains. Another antiviral drug zanamivir is shown to have better interaction than oseltamivir even compared to sialic acid.

Zanamivir interacts with seven amino acid residues of the NA whereas oseltamivir only interacts with two amino acid residues of the NA. This is possible because the structure of zanamivir is more similar to the sialic acid compared to oseltamivir. Interaction of DANA with NA is also quite good but due to its lower affinity compared with the sialic acid, DANA is considered not being able to compete with it. The interaction of RWJ-270 201 is not good enough because it interacts with only four amino acid residues of the NA.

Ligand screening based on energy association and contact residues

The results of ligand docking are 244 new designs. Screening would be done based on binding energy and the contact residues. The bond energy and the contact residues were compared with the bond energy results and the contact residues resulting from the standard docking. Thus, the ligand is considered to have better bond energy and contact residues than the standards which adhere to the following criteria:

1. Value of ΔG° (binding affinity) should be ≤ -7.4 Kcal/mol.
2. Occurred contact residues have at least four hydrogen bonds with three interactions with amino acid residues on the NA active side.

The ligands that pass screening based on binding energy and the contact residues are shown in Tables 3 and 4. It can be seen that out of 224 created designs, it was obtained that eight ligands have better affinity than the standard, four designs from the design based on structure and the four ligands from the entry blockers ligand based design. Further discussion will be conducted between the eight ligands comparisons with the standard ligand.

Energy association and inhibition constants (Ki)

As previously described the bond energy (ΔG°) shows affinity of ligands that bind to the enzyme to form complexes. Examining the value of the bond energy, we comprehend that the stability of ligand-enzyme complex is formed. Bond energy is also directly related to the inhibition constants or dissociation constants (K_i) which also could give an idea about the affinity between ligand

Table 3. The results of ligand screening (structure based design).

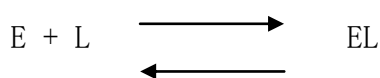
No.	Ligand	ΔG° binding affinity (kcal/mol)	Contact residue
1	DNY	-8.4	SER 247, GLU 278 , GLU 278 , TYR 402 , ARG 293 , ARG 293
2	NNY	-8.7	GLU 278 , TYR 402 , SER 247, ARG 293 , ARG 293 , TYR 402
3	DYY	-7.6	SER 247, SER 247, ARG 293 , ARG 368 , TYR 402
4	DDY	-8.4	ASP 151, GLU 278 , TYR 402 , SER 247, ARG 293 , ARG 293 , TYR 402 , TYR 402

Values in bold print are the targeted residue.

Table 4. The results of ligand screening (entry blocker).

No.	Ligand	ΔG° binding affinity (kcal/mol)	Contact residue
1	RRR	-8.0	GLU 278 , GLU 278 , GLU 278 , TYR 402 , TYR 402 , SER 247, ARG 368 , ARG 368
2	RRP	-8.0	GLU 278 , TYR 402 , TYR 402 , ARG 152, ARG 152, SER 247, ARG 293
3	RPR	-8.5	SER 247, GLU 278 , TYR 402 , ARG 293 , ARG 368 , ARG 368
4	LRL	-7.9	ILE 149, GLU 278 , TYR 402 , ARG 152, SER 247, ARG 293

Values in bold print are the targeted residue.



$$K_i = \frac{[E][L]}{[EL]}$$

$$[EL]$$

and enzyme. K_i formulated as follows:

Where, E is an enzyme, L is the ligand and the EL is an enzyme-ligand complexes. The smaller the value of K_i is, the more the equilibrium reaction will tend to lead to the formation of the complex. Enzyme-ligand complex is said to have a good affinity bond if it has a K_i value in the micro molar scale. Here is a comparison of bond energy values, and inhibition constants between ligand and standards that passed the previous screening.

It can be seen from Table 5 that all the ligands have an estimated value of K_i in the micromolar scale. pK_i means the mean value of logarithmic K_i value. The greater the value of the pK_i is, the smaller the value of K_i . From the data shown in Table 5, the ligands that have better value than standard pK_i are DNY, RRR, RRP, RPR and LRL.

From Table 5, it can also be known that the relationship between the value of the bond energy (ΔG°) with K_i is likely directly proportional and inversely when compared with the value of pK_i . It follows the formulated thermodynamic equation as follows:

$$\Delta G_o = -RT \ln K_i$$

Contact residues

The interaction between the ligand and the enzyme became one of the necessary parameters to determine the activity of a ligand to the enzyme. The target of the ligand interactions of the NA enzyme in this regard is the amino acid residues found on the NA active side. This is necessary because the ligand is expected to be created as NA inhibitors that have enzymatic functions. From the previous determination, it has been known that there are seven amino acid residues at the NA active side. They are Arg118, Asp151, Glu278, Arg293, Arg368, Tyr402 and Glu245. The more interaction, the greater the score of ligand interaction with amino acid residues of NA active site is. It is expected that inhibition of ligand function would be better. Ligand interactions that occur between the NA and inhibitor are hydrogen bond interaction with a

Table 5. Energy bonds and inhibition constants.

Ligand	ΔG° binding affinity(kcal/mol)	Pki
Oseltamivir	-6.5	12.122
Zanamivir	-7.4	11.628
DANA	-6.7	9.695
RWJ-270201	-6.8	11.275
DNY	-8.4	12.648
NNY	-8.7	8.048
DYY	-7.6	9.564
DDY	-8.4	9.780
RRR	-8.0	16.698
RRP	-8.0	18.789
RPR	-8.5	13.779
LRL	-7.9	13.468

Table 6. Residues and interaction contacts with the standard score of amino acid residues in the active side.

No.	Standard	Interaction score with catalytic site residue (%)						
		Arg 118	Asp 151	Glu 278	Arg 293	Arg 368	Tyr 402	Glu 425
1.	Sialic acid	-	-	32.8	38.7, 55.2, 49.1	-	10.6, 10.6	-
2.	DANA	-	14.1	22.6, 31.2	14.7	-	13.4, 44.0, 44.0	-
3.	Zanamivir	-	17.9, 34.4	14.2	-	25.1	61.0, 61.0, 89.0	-
4.	Oseltamivir	-	-	-	89.3	-	28.1	-
5.	RWJ-270201	-	20.0	31.6	-	-	-	-

Table 7. Contact residues and ligand interaction scores with the active side of the amino acid residues.

No.	Ligand	Interaction score with catalytic site residue (%)						
		Arg 118	Asp 151	Glu 278	Arg 293	Arg 368	Tyr 402	Glu 425
1	DNY	-	-	72.8	42.3, 21.1	-	32.2	-
2	NNY	-	-	14.8	53.5, 20.2	-	52.0, 21.4	-
3	DYY	-	-	-	29.5	25.8	28.1	-
4	DDY	-	11.5	14.1	53.4, 22.9	-	70.6, 21.5, 70.6	-
5	RRR	-	-	23.3, 22.9, 13.3	-	37.4, 33.2	11.4, 10.7	-
6	RRP	-	-	16.9	28.2	-	37.2, 37.2	-
7	RPR	-	-	11.0	39.7	13.0, 12.9	20.6	-
8	LRL	-	-	17.7	22.5	-	62.5	-

bond distance of at least 2.5 to 3.5 Å.

Table 6 shows contact residues and ligand interaction scores of the standard. From the standard ligand contact residue with the amino acid residues of the NA active site, oseltamivir and RWJ-270 201 only interact with two of the seven amino acid residues in the NA active site. Although score (89.3%) from the NA interaction with Arg293 is large enough, it is not enough to prove that oseltamivir still has good activity as an antiviral drug for influenza virus, because the affinity of oseltamivir against NA that has been previously known was very low. It is even lower than the sialic acid which theoretically would

tend to cause NA to bind to sialic acid compared to oseltamivir. Other standard ligands have seven interactions with amino acid residues on the active side of the interaction of NA with a good score. Table 7 shows contact residues and interaction score with amino acid residues at the NA active site. Eight ligands from Table 7 passed the previous screening. It can be seen that each ligand has at least three interactions with amino acid residues on the active side of the interaction of NA with a pretty good score. Although the standard, DANA, zanamivir and contact residues results have a better interaction score compared to others, it is seen from the

Table 8. The results of screening a ligand based drug likeness (drug scan).

No.	Ligand	Molecular weight (dalton)	H-bond donor	H-bond acceptor	LogP	Molar refractivity (optional)
1	*Oseltamivir	312,00	3	5	1,309	84,245
2	*Zanamivir	332,00	9	9	-6,657	75,831
3	*DANA	291,00	6	7	-7,814	62,861
4	*RWJ-270201	314,00	7	6	-2,588	80,929
5	DNY	598,00	10	9	-2,678	156,365
6	NNY	597,00	11	9	-1,97	146,536
7	DYY	647,00	9	10	-1,212	162,286
8	DDY	599,00	9	11	-3,148	142,352
9	RRR	674,00	18	15	-4,601	175,187
10	RRP	615,00	13	12	-3,358	158,839
11	RPR	615,00	13	12	-3,007	157,898
12	LRL	588,00	10	9	-1,042	155,793

*Standard; bold, did not pass screening.

determination results of the ligand affinity, that the previous eight have a better affinity than all the standards. It is an indication that residence time of the bond between the ligand and NA is better. It will also affect the use of concentration in the wet lab test later, that a ligand that has a better residence time requires less concentration of the ligand to inhibit an enzyme such as NA.

Screening ligand based drug likeness (drug scan)

The selected eight ligands are based on docking analysis (affinity and interaction). Out of them, there would be selected several ligands that have properties in common with an existing drug (drug likeness) using Lipinski's rules (Lipinski's rule of five) (Lipinski et al., 2001). Lipinski's rule of five is helpful to distinguish between molecules of drug-like and non drug like by taking into account the extent of absorption or permeability of lipid bilayer present in the human body. These rules predict the probability of determining drug-likeness of a molecule that has two or more criteria as follows:

1. The molecular weight of less than 500 mg/mol
2. Has a high lipophilicity (logp less than 5)
3. Hydrogen bond donors less than 5
4. Hydrogen bond acceptor is less than 10
5. Refractory molar between 40-130 (optional) (SCFBIO-IITD)

The result of ligand screening based on the drug likeness by using online software Lipinski's filter (SCFBIO-IITD) is shown in Table 8. From the data shown in Table 8, oseltamivir, which was used as a standard as well as antiviral drug commercially, had a graduation rate of four out of the five criteria based on Lipinski's rule of five,

which is the highest. While, zanamivir is also an antiviral drug that has been used commercially, having met three out of five Lipinski's rules criteria. The standard inhibitor DANA and RWJ-270 201 have the same criteria as zanamivir; three of the five criteria of Lipinski's rules are met. It means that they are having a sufficient level of drug likeness. Out of the screened eight ligands (docking analysis), only three ligands met two out of the Lipinski's five rules. They are DNY, NNY and LRL. It is because, the rules of Lipinski itself state that a molecule which has a good drug likeness should have at least two of the five criteria. The three ligands (DNY, NNY, and LRL) have quite good drug likeness levels and further analysis will be conducted on them.

The performed screening is still associated with the bioavailability level of oral drug likeness. High oral bioavailability is often an important consideration for developing bioactive molecules as therapeutic agent (Veber et al., 2002; Tambunan and Wulandari, 2010c). Oral bioavailability is the extent to which a drug or other substances will be available to the target tissue after administration of drugs or substance (Tambunan and Wulandari, 2010c). Screening levels of ligand oral bioavailability is based on two rules, namely Veber's rules (Veber et al., 2002) and Egan's rules (Egan et al., 2000). Veber's rules stated that oral bioavailability of drugs is good if it meets the following criteria:

1. Rotatable bonds is less than or equal to 10.
2. Topological polar surface area (tPSA) is less or equal with 140 Å.
3. Total H- bonds and H- acceptor of less than or equal to 12.

Egan's rules of a molecule stipulated that the oral bioavailability of drugs is good if it meets the following

Table 9. The results of oral bioavailability standard and ligand screening (Veber's Rules).

No.	Ligand	H-bond donor + H-bond acceptor (optional)	tPSA (Å)	Rotatable bond
1	*Oseltamivir	8	90,660	8
2	*Zanamivir	18	198,217	7
3	*DANA	13	156,543	5
4	*RWJ-270201	13	148,527	7
5	DNY	19	260,107	7
6	NNY	20	265,902	7
7	DYY	19	237,241	7
8	DDY	20	254,312	7
9	RRR	33	345,192	16
10	RRP	25	274,501	11
11	RPR	25	274,501	11
12	LRL	19	221,388	10

*Standard; bold, did not pass screening.

criteria:

1. $0 \geq \text{tPSA} \leq 132 \text{ \AA}$.
2. $-1 \geq \text{LogP} \leq 6$.

Screening is done by determining the ligand properties, using the online software molinspirations (molinspirations.com) to examine some properties of ligands such as tPSA, logP and number of rotatable bonds (nortb). The results of oral bioavailability of standard screening and ligand are seen in Tables 9 and 10. Oral bioavailability screening results showed that only oseltamivir meets all the criteria based on Veber's and Egan's rules. For zanamivir, which is one of the antiviral drugs, it did not meet criteria based on the oral bioavailability of Veber's and Egan's rules, as well as two standard inhibitors (DANA and RWJ-270201). Most of the ligand designs also have the same criteria with zanamivir, on the grounds that oral bioavailability is not a guarantee to distinguish drug-like and non drug-like molecules. Based on the screening results (Lipinski's rule of five and oral bioavailability screening), the ligands designs that have the best drugs likeness are DNY, NNY and LRL.

Visualization of enzyme-ligand complex interactions

The interaction between the ligand with the enzyme was visualized using two different offline softwares. They are PyMol and MOE2008.10. PyMol can display 3D high resolution images and can be designed according to desired needs, while MOE 2008.10 interaction picture was displayed in the form of 2D image with bonding parameters that have been determined automatically. From Figures 2, 3 and 4, it can be seen that the visualization of complex enzyme-ligand interactions of the

three new ligand designs are DNY, NNY and LRL using PyMol software. From the image A, it can be seen that the interaction between the ligand with NA, red lines indicate hydrogen bonding that occurs between the ligand with NA; whereas for image B, it can be seen with the surface of the ligand cavity or pocket of the catalytic site (active side) of NA. In the images, it could be seen whether the structure of the ligand is appropriate or sufficient to form a pocket in the NA active site.

The ligand structure of NNY and DNY are quite fit to the shape of the NA active site side pocket and it is visible; also both ligand aromatic groups occupy a crevice that is quite appropriate, so the aromatic group is still large enough to enter the active side of the NA. Whereas, ligand LRL has a structure larger than DNY and NNY, so it does not quite match the shape of the NA active side pocket. It can be seen that there are enough side chains of arginine (R) so that the ligand slightly pushes out of the pocket side of the NA active site. Here is a visualization of the enzyme-ligand interactions using the software MOE 2008. 10;

1. DNY ligand interaction with NA in Tables 8 and 9 show some interactions between amino acid residues at the NA active site with the ligand through hydrogen bonding, which occurred with the Tyr 402, Arg293, Glu278 side chains of asparagines (N) and aspartic acid (D) that is, asetamine and carboxyl. However, it can be seen that the interaction of the amino acids Arg368 to the center or core of the aromatic groups exists on the ligand (Figure 5).

2. NNY ligand interactions with NA are similar to DNY ligand interactions with NA, but there are differences in amino acid residues that interact with the aromatic core of the group. While on NNY, it is Arg225, and on DNY, it is Arg368. This is due to different ligand conformation

Table 10. The results of oral bioavailability standard and ligand screening (Egan's Rules).

No.	Ligand	LogP	PSA (Å)
1	*Oseltamivir	1.309	90.660
2	*Zanamivir	-6,657	198,217
3	*DANA	-7,814	156,543
4	*RWJ-270201	-2,588	148,527
5	DNY	-2,678	260,107
6	NNY	-1,970	265,902
7	DYY	-1,212	237,241
8	DDY	-3,148	254,312
9	RRR	-4,601	345,192
10	RRP	-3,358	274,501
11	RPR	-3,007	274,501
12	LRL	-1,042	221,388

*Standard; bold, did not pass screening.

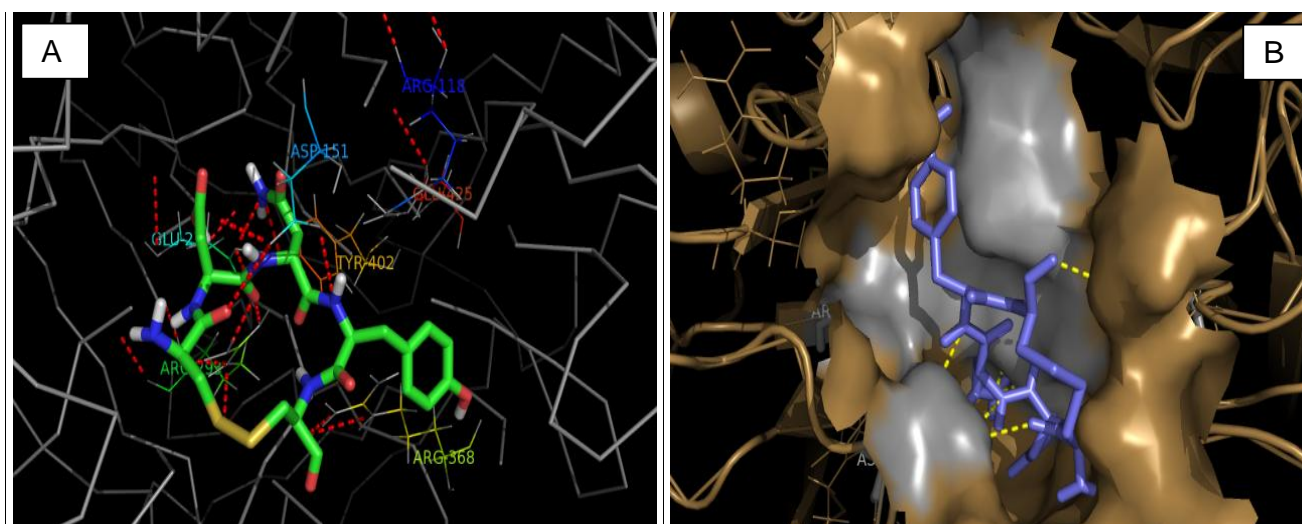


Figure 2. 3D Interaction of Ligand DNY with NA.

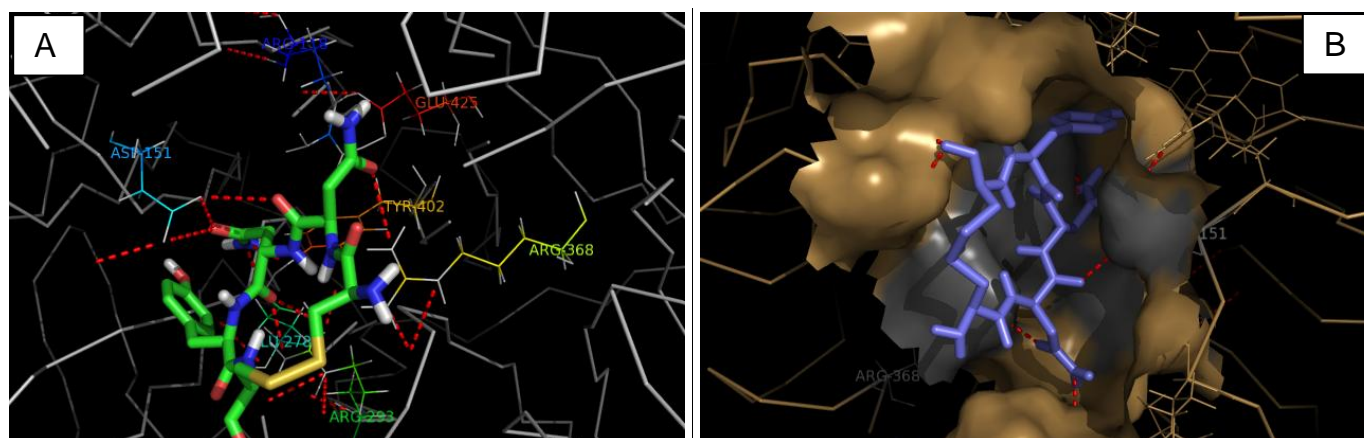


Figure 3. 3D Interactions of Ligand NNY with NA.

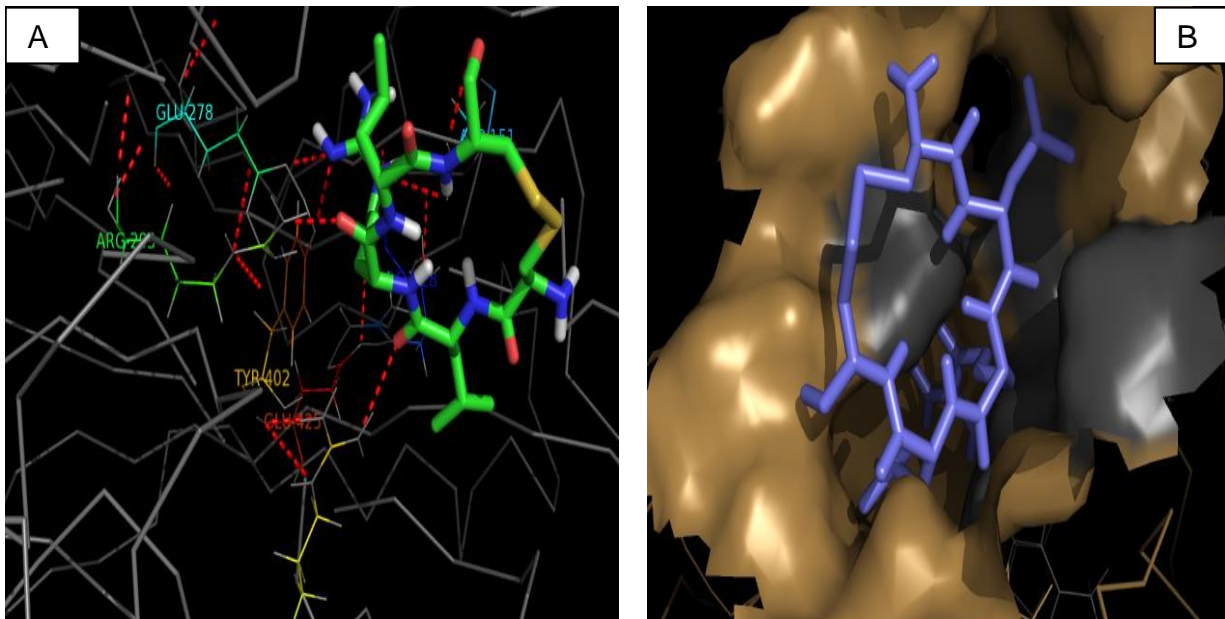


Figure 4. 3D Interaction of Ligand LRL with NA.

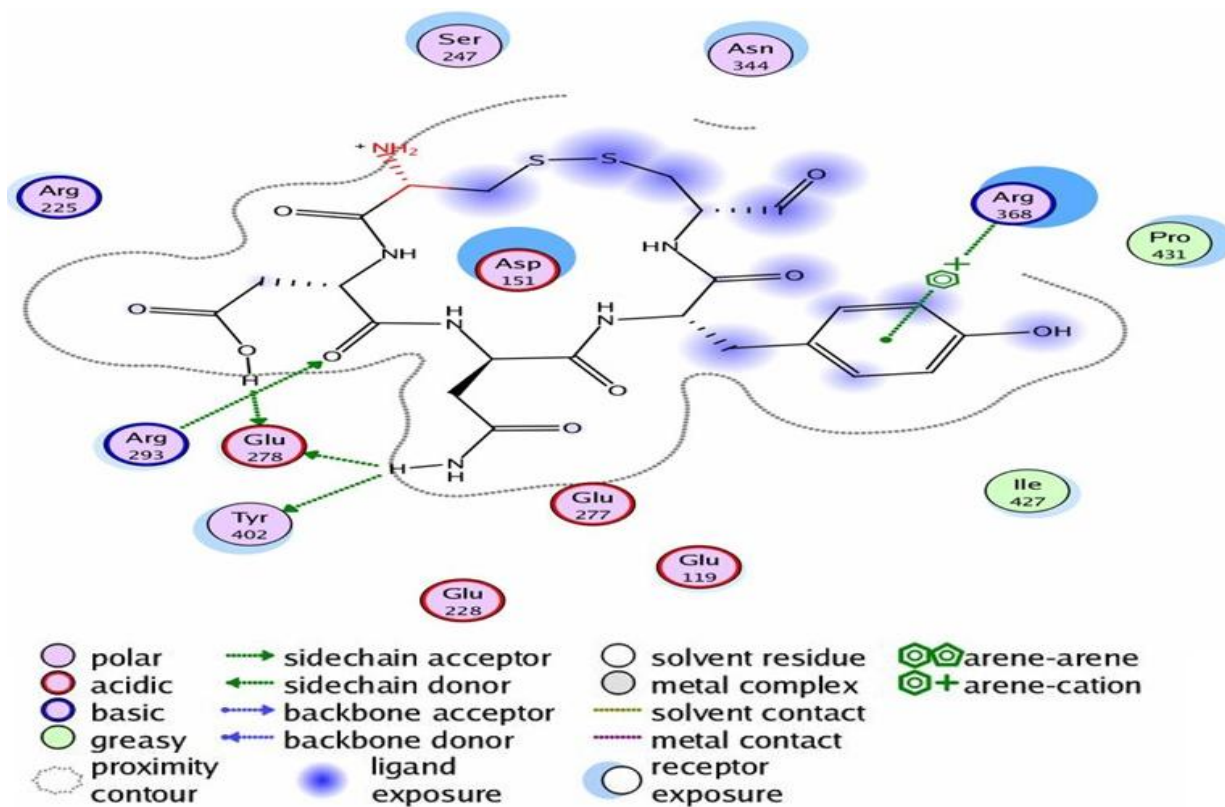


Figure 5. 2D DNY ligand interactions with NA.

between DNY and NNY; the interaction through hydrogen bonding mostly happens with the side chain of asparagine (N) amino acid residue. It is the acetamine

group (Figure 6).

3. LRL ligand interactions with NA have more evenly distributed hydrogen bonds with amino acid residues at

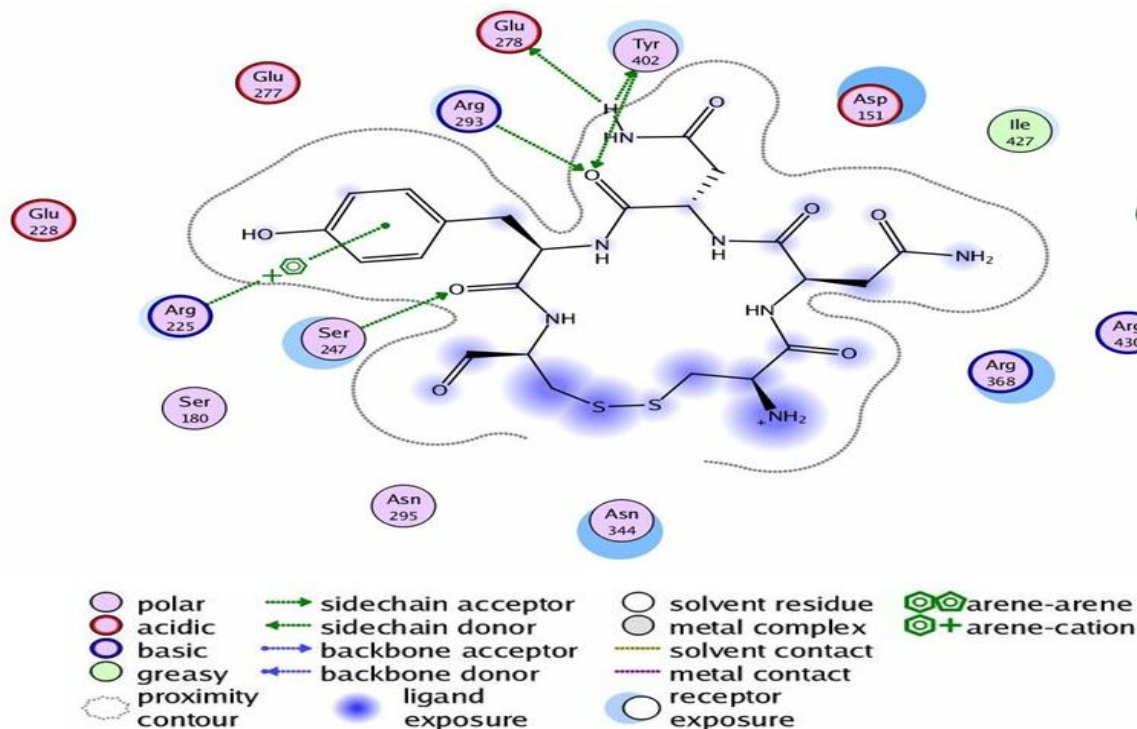


Figure 6. 2D NNY ligand interactions with NA.

the NA active site than NNY and DNY. Both of them are more focused on the carboxyl group and a setamine. Visible side chain of arginine is also large enough to have a pretty good interaction with Tyr402 and Glu278; despite the previous 3D visualization of the arginine side chain causing the ligand to be slightly pushed out of the pocket side of the NA active site (Figure 7).

Toxicological properties

A determination method for the molecules toxicological properties in the development of drug design is getting more important. It is necessary to predict drugs adverse effects on living being. This development involves several aspects and methods that can be adopted from various existing types of research. One method that can be used in this toxicology study is quantitative structure-activity relationship (QSAR). Animals testing data are the basis of QSAR which cannot guarantee the completeness of the data required for the toxicology studies. Studies using animals have some limitations such as funding, the long required time, the unavailability of adequate laboratory, inability to generate insufficient data, and a problem of ethics in the use of animals as test material. These problems could be overcome by developing several tools that can perform toxicology studies or determination of the toxicological properties of a molecule quickly and cost-effective. Some software has been developed to assist investigators in determining the toxicological

properties of a molecule, for examples:

1. Toxtree (Ideacon Ltd., Bulgaria).
2. Lazar (<http://lazar.in-silico.de/>).

Both the software above was utilized in determining the toxicological properties of all three ligands from the screening results; they are DNY, NNY and LRL.

Determination of the toxicological properties of the three ligands are focused on the carcinogenicity and mutagenicity which serve as an important concern in human health and deal directly with the ligand which is a cardinal goal of drug design. The difference between the softwares is the basis for determining the toxicological properties of a molecule. Toxtree is based on the rules of Benigni/Bossa for mutagenicity and carcinogenicity (Benigni and Bossa, 2008) (from the Instituto Superiore Sanita, Rome, Italy, and approved by the European Chemical Bureau, Institute for Health and Consumers Protection, European Commission-Joint Research Centre (JRC) in 2008). Some points to consider in determining the toxicological properties using ToxTree for instance are the presence or absence of a structural alert (SAS) that is genotoxic and nongenotoxic and determination of the QSAR.

Lazar online software is based upon the structural equation fragment of the observed molecule. The nature of the structural fragment that exists in toxicology databases for known carcinogenicity and mutagenicity was based on the test results using laboratory animals

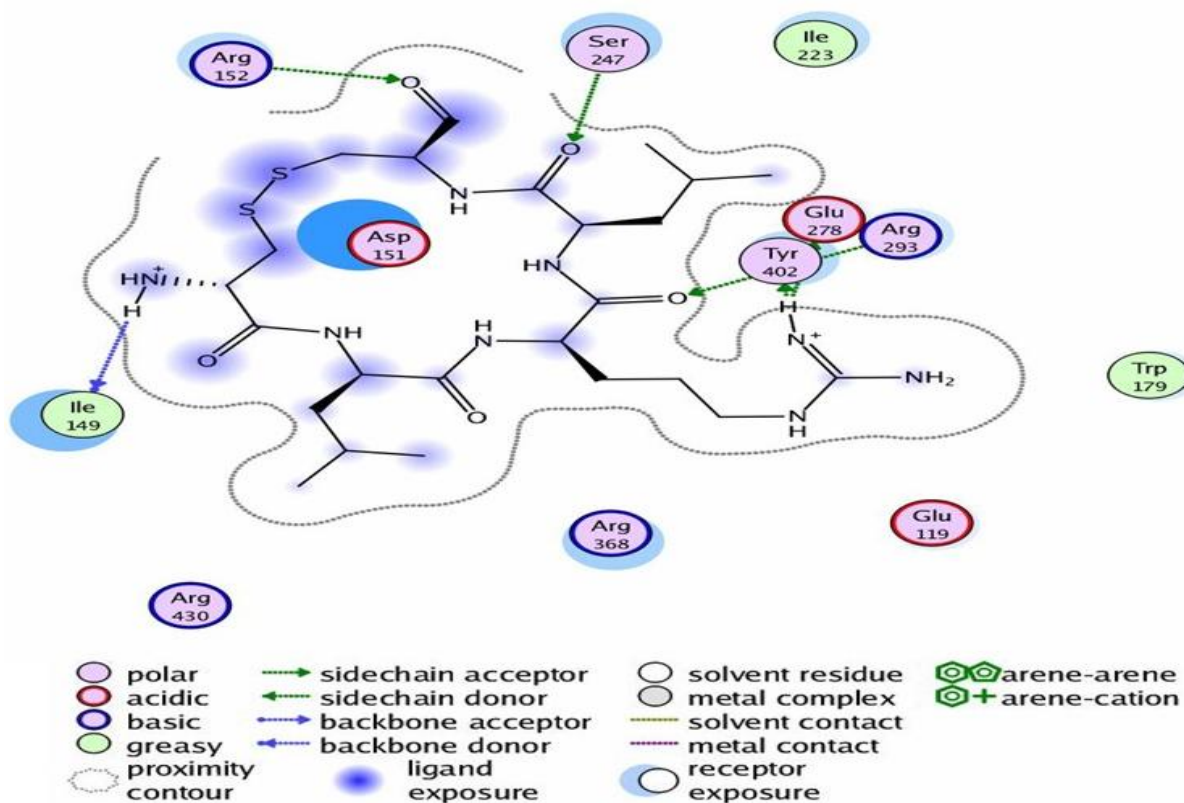


Figure 7. 2D ligand interactions LRL with neuraminidase.

Table 11. Toxtree toxicity prediction results.

Toxtree toxicity prediction	DNY	NNY	LRL
Structural alert for genotoxic carcinogenicity	No	No	No
Structural alert for nongenotoxic carcinogenicity	No	No	No
Potential carcinogen based on QSAR	No	No	No
Potential <i>S. typhimurium</i> TA100 mutagen based on QSAR	No	No	No
Negative for genotoxic carcinogenicity	Yes	Yes	Yes
Negative for nongenotoxic carcinogenicity	Yes	Yes	Yes

and microbial (Ames test). The result of the determination of toxicological properties by using both softwares is seen in Tables 11 and 12. From the results of toxicological prediction using software Toxtree, those three ligands have no structural alerts (SAS) that are genotoxic and nongenotoxic, and also with the QSAR approach was detected as not mutagenic and carcinogen. While the results are predictable, Lazar software detected mutagenic properties of the three ligands on *Salmonella typhimurium* by two methods. They are CPDB and Kazius/Bursi, and apparently only the active or positive LRL is predicted to be mutagenic in *S. typhimurium* (Kazius/Bursi). The carcinogens are predicted using test animals of the rodent, rat, murine and hamsters with regard to the gender; it is only the LRL that is predicted to

be active or positive carcinogens on hamsters. Some parameters in the software Lazar do not show the results (not available) of the three ligands which are caused by the data that have structural similarities with fragment. It has less supported entry, and it is not enough to predict the outcome of those parameters such as LC50 and the daily dose.

Synthetic accessibility (SA)

Ligands shown to have a good affinity to target enzyme do not have a practical value, if the design could not be synthesized by wet lab. Therefore, to help predict whether a designed molecules/ligands could be synthe-

Table 12. Lazar toxicity prediction results.

Lazar toxicity prediction	Predicted activity		
	DNY	NNY	LRL
96 h LC50	Not available	Not available	Not available
Human liver toxicity - Composite activity	Not available	Not available	Not available
Human liver toxicity - GGT increase	Not available	Not available	Not available
Human liver toxicity - LDH increase	Not available	Not available	Not available
Human liver toxicity - SGOT increase	Not available	Not available	Not available
Human liver toxicity - SGPT increase	Not available	Not available	Not available
Mutagenicity - Salmonella typhimurium (CPDB)	Inactive	Inactive	Inactive
Mutagenicity - Salmonella typhimurium (Kazius/Bursi)	Inactive	inactive	Active
Rodent carcinogenicity (multiple sex/species/sites)	Inactive	Inactive	Inactive
Rodent carcinogenicity (single sex/species/site)	Inactive	Inactive	Inactive
Rat carcinogenicity (both sexes)	Inactive	inactive	Inactive
Rat carcinogenicity (male)	Inactive	inactive	Inactive
Rat carcinogenicity (female)	Inactive	inactive	Inactive
Mouse carcinogenicity (both sexes)	Inactive	inactive	Inactive
Mouse carcinogenicity (male)	Inactive	inactive	Inactive
Mouse carcinogenicity (female)	Inactive	inactive	Inactive
Hamster carcinogenicity (both sexes)	Inactive	inactive	Active
Hamster carcinogenicity (male)	Inactive	inactive	Inactive
Hamster carcinogenicity (female)	Inactive	Inactive	Active
IRIS upper-bound excess lifetime cancer risk	Not available	Not available	Not Available
FDA maximum recommended daily dose (FDAMDD)	Not available	Not available	Not Available

Table 13. The results of the SA prediction.

Ligand	Structural complexity (%)	Starting materials (%)	Synthetic accessibility (%)
*Oseltamivir	32	49	62
*Zanamivir	10	92	89
DNY	41	76	58
NNY	41	76	58
LRL	39	77	60

Description*: Ligand standard (antiviral drug).

sized by wet-lab or not, parameter called synthetic accessibility (SA) should be applied. It has provided online software that helps to determine the SA. The name is CAESA, which was developed by Symbiosis Inc. and supported by Keymodule Ltd, Leeds, UK and Pfizer. The basis of the SA determination is using the structural complexity CAESA of these molecules and the availability of starting materials to synthesize such molecules as seen from the databases Across, Aldrich and Lancaster. Prediction of the three synthetic ligands accessibility of DNY, NNY and LRL and oseltamivir and zanamivir are merupakan antiviral drug that has been used commercially as a comparison (Table 13).

Zanamivir, as a commercial antiviral drug, has a high SA score of 89% because its structure is not too complex (10%) and has adequate availability of starting materials

(92%), while the SA score for oseltamivir is 62% because its availability of starting materials is only 49%. It can be quite low because oseltamivir is been used commercially as zanamivir. For all three ligands, DNY and NNY have the same structural complexity, which is 41 and 76% availability of the starting materials, so that the SA score for the second ligand is about 58%. It is because the structure is similar to NNY and DNY, distinguished only by one amino acid residue D (aspartic acid) and N (asparagine); while, the LRL has structural complexity lower than DNY and NNY at 39% with the availability of starting materials of 77%. SA score of LRL is greater than NNY and DNY (60%), when compared with predicted results for synthetic ligands accessibility of the three ligands. DNY, NNY and LRL are likely to be able to be synthesized in the wet lab because the SA score does

not have much difference from oseltamivir, which has been synthesized on a large scale for commercial needs. Although all three structures in terms of ligand are more complex than oseltamivir, the availability of starting materials of them can be said to be more numerous and easier than oseltamivir.

Conclusion

Oseltamivir, as one of the antiviral drug for influenza virus subtype H1N1 NA, loses its activity due to mutations of the NA itself, while zanamivir is still having good activity in the enzymatic function of NA inhibition. From the results of docking, Oseltamivir, DANA and RWJ-270 201 ΔG° values were greater than the NA natural substrate of sialic acid. Henceforth, we can conclude that the NA theoretically would be more likely to bind to sialic acid for enzyme-ligand complexes formation. It will be more stable. From the results of molecular docking and drug scan based on Lipinski's rule of five and oral bioavailability rules (Egan's and Veber's rules), the best of the three candidates ligand DNY, NNY and LRL was elucidated.

Toxicological properties of NNY and DNY ligands were predicted as non-carcinogens and non-mutagens. Only ligand LRL is predicted to be mutagens with the use of *S. typhimurium* (Kazius/Bursi) and carcinogens in female test animals. Ligand DNY and NNY have SA score of 58%, while LRL, 60%. Those ligands designs are likely to be synthesized by wet lab. Molecular dynamic simulation needs to be done to determine the effect of temperature and solvent on the interaction of ligands with NA and there is need to carryout absorption, distribution, metabolism and excretion (ADME) analysis and bioactivity of the ligand that has been designed to determine the treatment of the human body against the ligand system that has been made.

ACKNOWLEDGEMENTS

This research was supported by Hibah Pasca Sarjana, Dikti, Ministry of Education and Culture, Republic of Indonesia. We are thankful to Ms. Samira Alamudi, The Departement of Chemical Biology, National University of Singapore, for her kind proof reading of the manuscript. The authors also thankful to Dr. Ridla Bakri, Chairman of Department of Chemistry, Faculty of Mathematics and Science University of Indonesia for supporting this research.

REFERENCES

Benigni R, Bossa C (2008). The Benigni/Bossa rulebase for mutagenicity and carcinogenicity a module of ToxTree. JRC scientific and technical reports. European Comission Joint Research Center.
 Binghe W, Siahaan T, Soltero R (2005). Drug Delivery: Principles and

Applications. John Wiley & Sons, Inc. Hoboken, New Jersey.
 Chen L, Feng KY, Cai YD, Chou KC, Li HP (2010). Predicting the network of substrate-enzyme-product triads by combining compound similarity and functional domain composition. BMC Bioinformatics, 11: 293.
 Chou KC (1993). A vectorized sequence-coupling model for predicting HIV protease cleavage sites in proteins. J. Biol. Chem., 268: 16938-16948.
 Chou KC (1996). Review: Prediction of HIV protease cleavage sites in proteins. Anal. Biochem., 233: 1-14.
 Chou KC (2004). Review: Structural bioinformatics and its impact to biomedical science. Curr. Medicinal Chem., 11: 2105-2134.
 Chou KC, Wei DQ, Zhong WZ (2003). Binding mechanism of coronavirus main proteinase with ligands and its implication to drug design against SARS. (Erratum: *ibid.*, 2003, Vol.310, 675). Biochem. Biophys. Res. Commun., 308: 148-151
 Chou KC (2001). Prediction of protein cellular attributes using pseudo amino acid composition. PROTEINS: Structure, Function, and Genetics, Erratum: *ibid.*, 44, 60(43): 246-255
 Chou KC, Shen HB (2008). Cell-PLoc: A package of Web servers for predicting subcellular localization of proteins in various organisms (updated version: Cell-PLoc 2.0: An improved package of web-servers for predicting subcellular localization of proteins in various organisms, Natural Science, 2010, 2, 1090-1103). Nat. Protocols, 3: 153-162.
 Chou KC, Shen HB (2008). ProtIdent: A web server for identifying proteases and their types by fusing functional domain and sequential evolution information. Biochem. Biophys. Res. Commun., 376: 321-325.
 Chou KC, Shen HB (2007). Signal-CF: a subsite-coupled and window-fusing approach for predicting signal peptides. Biochem. Biophys. Res. Commun., 357: 633-640.
 Chou KC, Shen HB (2007). MemType-2L: A Web server for predicting membrane proteins and their types by incorporating evolution information through Pse-PSSM. Biochem. Biophys. Res. Commun., 360: 339-345.
 Chou KC, Wu ZC, Xiao X (2011). iLoc-Euk: A Multi-Label Classifier for Predicting the Subcellular Localization of Singleplex and Multiplex Eukaryotic Proteins. PLoS One, 6: e18258.
 De Clercq E (2006). Antiviral agents active against influenza A virus. Nat. Rev. Drug Discov., 5: 1015-1025.
 De Jong MD, Thanh TT, Khanh TH, Hien VM, Smith GJD, Chau NV, Cam BV, Qui PT, Ha DQ, Guan Y, Peiris JSM, Hien TT, Farrar J (2005). Oseltamivir resistance during treatment of influenza A (H5N1) infection. N. Engl. J. Med., 353(25): 2667-2672.
 Du QS, Wei H, Huang RB, Chou KC (2011). Progress in structure-based drug design against influenza A virus. Expert Opin., 6: 619-631.
 Du QS, Wang SQ, Huang RB, Chou KC (2010). Computational 3D structures of drug-targeting proteins in the 2009-H1N1 influenza A virus. Chem. Phys. Lett., 485: 191-195.
 Du QS, Huang RB, Wang SQ, Chou KC (2010). Designing inhibitors of M2 proton channel against H1N1 swine influenza virus. PLoS ONE, 5: e9388.
 Du QS, Huang RB, Wang CH, Li XM, Chou KC (2009). Energetic analysis of the two controversial drug binding sites of the M2 proton channel in influenza A virus. J. Theor. Biol., 259: 159-164.
 Du QS, Wang SQ, Chou KC (2007). Analogue inhibitors by modifying oseltamivir based on the crystal neuraminidase structure for treating drug-resistant H5N1 virus. Biochem. Biophys. Res. Commun., 362: 525-531.
 Egan WJ, Merz KM, Baldwin JJ (2000). Prediction of Drug Absorption Using Multivariate statistic. J. Med. Chem., 43: 3867-3877.
 European Chemical Agency (2008). Guidance on information requirements and chemical safety assessment Chapter R.6: QSARs and grouping of chemicals.
 Gong K, Li L, Wang JF, Cheng F, Wei DQ (2009). Binding mechanism of H5N1 influenza virus neuraminidase with ligands and its implication for drug design. Med. Chem., 5: 242-249.
 Guo XL, Li L, Wei DQ, Zhu YS, Chou KC (2008). Cleavage mechanism of the H5N1 hemagglutinin by trypsin and furin. Amino Acids, 35: 375-382.

- He Z, Zhang J, Shi XH, Hu LL, Kong X (2010). Predicting drug-target interaction networks based on functional groups and biological features. *PLoS ONE*, 5: e9603.
- Hu LL, Chen C, Huang T, Cai YD, Chou KC (2011). Predicting biological functions of compounds based on chemical-chemical interactions. *PLoS ONE*, 6: e29491.
- Hu LL, Huang T, Cai YD, Chou KC (2011). Prediction of Body Fluids where Proteins are Secreted into Based on Protein Interaction Network. *PLoS One*, 6: e22989.
- Huang RB, Du QS, Wang CH, Chou KC (2008). An in-depth analysis of the biological functional studies based on the NMR M2 channel structure of influenza A virus. *Biochem. Biophys. Res. Commun.*, 377: 1243-1247.
- Huang T, Niu S, Xu Z, Huang Y, Kong X (2011). Predicting Transcriptional Activity of Multiple Site p53 Mutants Based on Hybrid Properties. *PLoS ONE*, 6: e22940.
- Huang T, Shi XH, Wang P, He Z, Feng KY (2010). Analysis and prediction of the metabolic stability of proteins based on their sequential features, subcellular locations and interaction networks *PLoS ONE*, 5: e10972.
- Jones JC, Turpin EA, Bultmann HB, Curtis R, Schultz-Cherry S (2006). Inhibition of Influenza Virus Infection by a Novel Antiviral Peptide That Targets Viral Attachment to Cells. *J. Virol.*, pp. 11960-11967.
- Kamps B, Hoffmann C, Preiser W (2006). *Influenza Report 2006*. Flying Publisher.
- Kubinyi H (1998). Structure-based design of enzyme inhibitors and receptor ligands. *Curr. Opin. Drug Discov. Dev.*, 1(1): 4-15.
- Lew W, Chen X, Kim CU (2000). Discovery and development of GS 4104 (oseltamivir): an orally active influenza neuraminidase inhibitor. *Curr. Med. Chem.*, 7(6): 663-672.
- Li XB, Wang SQ, Xu WR, Wang RL, Chou KC (2011). Novel Inhibitor Design for Hemagglutinin against H1N1 Influenza Virus by Core Hopping Method. *PLoS One*, 6: e28111.
- Lipinski CA, Lombardo F, Dominy BW, Feeney PJ (2001). Experimental and computational approaches to estimate solubility and permeability in drug discovery and development setting. *Adv. Drug. Del. Rev.*, 46: 3-26.
- Michaelis M, Doerr HW, Cinatl J (2009). An influenza A H1N1 virus revival pandemic H1N1/09 virus. *Infection*, 5: 381-389.
- Pielak RM, Chou JJ (2010). Kinetic analysis of the M2 proton conduction of the influenza virus. *J. Am. Chem. Soc.*, 132: 17695-17697.
- Pielak RM, Jason R. Schnell JR, Chou JJ (2009). Mechanism of drug inhibition and drug resistance of influenza A M2 channel. *Proceed. Natl. Acad. Sci., USA*, 106: 7379-7384.
- Rungrotmongkol T, Intharathep P, Malaisree M, Nunthaboot N, Kaiyawet N, Sompornpisut P, Payungporn S, Poovorawan Y, Hannongbua S (2009). Susceptibility of antiviral drugs against 2009 influenza A (H1N1) virus. *Biochem. Biophys. Res. Commun.*, 385(3): 390-394
- Schnell JR, Chou JJ (2008). Structure and mechanism of the M2 proton channel of influenza A virus. *Nature*, 451: 591-595.
- Tomassini J, Selnick H, Davies ME, Armstrong ME, Baldwin J, Bourgeois M, Hastings J, Hazuda D, Lewis J, McClements W (1994). Inhibition of cap (m7GpppXm)-dependent endonuclease of influenza virus by 4-substituted 2,4-dioxobutanoic acid compounds. *Antimicrob Agent Chemother.*, 38: 2827-2837.
- Toxic User Manual (2008). Experimental and Computational Carcinogenesis Unit Environment and Health Department Istituto Superiore di Sanita' Viale Regina Elena 299 00161 Rome Italy.
- Young D, Fowler C, Bush K (2001). RWJ-270201 (BCX-1812): a novel neuraminidaseinhibitor for influenza. *Philos Trans. R. Soc. Lond. B Biol. Sci.*, 356(1416): 1905-1913.
- Veber DF, Johnson SR, Cheng HY, Smith BR, Ward KW, Kopple KD. (2002). Molecular Properties that Influence the oral Bioavailability of drug Candidates. *J. Med. Chem.*, 47(1): 224-232.
- Wang J, Pielak RM, McClintock MA, Chou JJ (2009). Solution structure and functional analysis of the influenza B proton channel. *Nat. Struct. Mol. Biol.*, 16: 1267-1271.
- Wang JF, Chou KC (2010). Insights from studying the mutation-induced allostery in the M2 proton channel by molecular dynamics. *Protein Eng. Des. Sel.*, 23: 663-666.
- Wang JF, Wei DQ, Chou KC (2009). Insights from investigating the interactions of adamantane-based drugs with the M2 proton channel from the H1N1 swine virus. *Biochem. Biophys. Res. Commun.*, 388: 413-417.
- Wang P, Hu L, Liu G, Jiang N, Chen X (2011). Prediction of antimicrobial peptides based on sequence alignment and feature selection methods. *PLoS ONE*, 6: e18476.
- Wang P, Xiao X, Chou KC (2011). NR-2L: A Two-Level Predictor for Identifying Nuclear Receptor Subfamilies Based on Sequence-Derived Features. *PLoS ONE*, 6: e23505.
- Wang SQ, Cheng XC, Dong WL, Wang RL, Chou KC (2010). Three new powerful Oseltamivir derivatives for inhibiting the neuraminidase of influenza virus. *Biochem. Biophys Res. Commun.*, 401: 188-191.
- Wang SQ, Du QS, Chou KC (2007). Study of drug resistance of chicken influenza A virus (H5N1) from homology-modeled 3D structures of neuraminidases. *Biochem. Biophys. Res. Commun.*, 354: 634-640.
- Wang SQ, Du QS, Huang RB, Zhang DW, Chou KC (2009). Insights from investigating the interaction of oseltamivir (Tamiflu) with neuraminidase of the 2009 H1N1 swine flu virus. *Biochem. Biophys. Res. Commun.*, 386: 432-436.
- Wei H, Wang CH, Du QS, Meng J, Chou KC (2009). Investigation into adamantane-based M2 inhibitors with FB-QSAR. *Med. Chem.*, 5: 305-317.
- Wei DQ, Du QS, Sun H, Chou KC (2006). Insights from modeling the 3D structure of H5N1 influenza virus neuraminidase and its binding interactions with ligands. *Biochem. Biophys. Res. Commun.*, 344: 1048-1055.
- Xiao X, Wang P, Chou KC (2011). GPCR-2L: Predicting G protein-coupled receptors and their types by hybridizing two different modes of pseudo amino acid compositions. *Mol. Biosyst.*, 7: 911-919.
- Zhang J, Wang Q, Fang H, Xu W, Liu A, Du G (2009). Design, synthesis, inhibitory activity and SAR studies of Pyrrolidine derivatives as neuraminidase inhibitors. *Bioorg. Med. Chem.*, 15(7): 2749-58
- Zhang Q, Yang J, Liang K, Feng L, Li S, Wan J, Xu X, Yang G, Liu D, Yang S (2008). Binding Interaction Analysis of the Active Site and Its Inhibitors for Neuraminidase (N1 Subtype) of Human Influenza Virus by the Integration of Molecular Docking, FMO Calculation and 3D-QSAR CoMFA Modeling. *J. Chem. Inf. Model.*, 48: 1802-1812.